Canadian Chemical Transactions

ISSN 2291-6458 (Print), ISSN 2291-6466 (Online)
Year 2014 | Volume 2 | Issue 1 | Page 83-96

Research Article

DOI:10.13179/canchemtrans.2014.02.01.0059

Research on the Batch and Fixed-Bed Column Performance of Red Mud Adsorbents for Lead Removal

Iman Mobasherpour*, Esmail Salahi and Ali Asjodi

Ceramics Department, Materials and Energy Research Center, P.O. Box 31787-316, Karaj, Iran

*Corresponding Author, E-mail: I.Mobasherpour@merc.ac.ir, Iman.Mobasherpour@gmail.com
Tel: +98(261)6204131*

Received: *November 5, 2013* ***Revised:*** *December 23, 2013* ***Accepted:*** *December 23, 2013* ***Published:*** *December 24, 2013*

Abstract: The removal of lead from water by red mud using batch and fixed-bed column adsorption techniques was investigated. In a batch study, experiments indicated that the time to attain equilibrium was 2h. The experimental data fitted well to a Langmuir adsorption isotherm and the adsorption capacity was 18.87 mg/g. Fixed-bed column experiments were carried out for different influent lead concentrations, bed depths, and various flow rates. The breakthrough time and exhaustion time decreased with increasing flow rate, decreasing bed depth and increasing influent lead concentration. The bed depth service time model and the Thomas model were applied to the experimental results. Both model predictions were in good agreement with the experimental data for all the process parameters studied, indicating that the models were suitable for red mud fix-bed column design.

Keywords: Red Mud; Pb^{2+} Contamination; Adsorption; Removal of Heavy Metal

1. INTRODUCTION

Water pollution is the contamination of water bodies such as lakes, rivers, oceans, and groundwater caused by human activities, which can be harmful to organisms and plants which live in these water bodies. Water pollution by toxic heavy metals through the discharge of industrial waste is a worldwide environmental problem. The presence of heavy metals in streams, lakes, and groundwater reservoirs has been responsible for several health problems with plants, animals, and human beings [1]. Heavy metal contamination exists in aqueous waste stream from many industries such as metal plating, mining, tanneries, painting, car radiator manufacturing, as well as agricultural sources where fertilizers and fungicidal spray are intensively used [2,3].

Lead is one of the most ubiquitous contaminants in the soil and aqueous environments. A severe environmental Pb contamination can often be found at shooting ranges where the soil Pb concentration sometimes exceeds 10000 mg kg^{-1} because of spent lead bullets. In Iran, many shooting ranges are generally located in mountainous regions and suffer from the degradation of natural vegetation due to Pb toxicity, which may have the potential to augment the Pb contamination via soil erosion. Therefore, development of cost-effective technologies is necessary to reduce the mobility and bioavailability of Pb in

ISSN 2291-6458 (Print), ISSN 2291-6466 (Online)
Year 2014 | Volume 2 | Issue 1 | Page 83-96

soil and water environments [4,5].

Studies proved that metals such as lead, copper, zinc, nickel, chromium, and mercury which have been considered as hazardous heavy metals are very toxic elements and they are commonly found in water and wastewater. So, the removal of these metals from wastewater is necessary. In wastewater treatment technology, various methods have been used to remove heavy metals from aqueous solutions. Traditional methods for the removal and recovery of heavy metals from industrial waste streams are precipitation, ion exchange, electrolysis, adsorption on activated carbon, etc. Most of these methods are extremely expensive or inefficient, especially for a large amount of solution at relatively low concentrations [6–9]. Among the various water-treatment techniques described, adsorption is generally preferred for the removal of heavy metal ions due to its high efficiency, easy handling, availability of different adsorbents and cost effectiveness. Recently, there has been an increasing emphasis on the adsorbent with low cost for the heavy metal ions removal. Most cases have also confirmed that the use of large quantities of such kind of wastes for the treatment of polluted water is an attractive and promising option with a double benefit for the environment [10–12].

Red mud emerges as a residue during alkaline-leaching of bauxite in Bayer process. Roughly 1–2 tons of red mud residues are produced for a ton of alumina [13]. Since the plant began to process, red mud has accumulated over years and causes a serious environmental problem due to its high alkalinity and large amount. Many have studied the application of red mud in wastewater treatment and red mud has been found to remove chromium [14], hexavalent [15], dyes [16], and heavy metals [17], from aqueous solution. Due to the high percentages of calcium, aluminum and iron, red mud is a good candidate for use as an economic adsorbent for large-scale use.

The present study sought to investigate Jajarm red mud as an alternative lead adsorbent. The objectives were to: (i) perform batch studies to examine lead adsorption using red mud (effect of initial lead concentration and adsorption isotherm) and (ii) perform column studies to investigate the lead uptake characteristics of red mud under different flow rates.

2. EXPERIMENTAL

2.1. Preparation of adsorbent

Red mud has been obtained as bauxite waste in the manufacture of alumina and emerges as unwanted by-products during alkaline-leaching of bauxite in Bayer process. The alkaline red mud-water pump has been dumped annually into specially constructed dams around the Jajarm Aluminum Plant (Jajarm, Iran). Red mud used in this experimental study has been obtained from this plant.

The alkaline red mud was thoroughly washed with distilled water until it became neutral. The suspension was wet sieved through a 200mesh screen. A little amount of the suspension remained on the sieve and was discarded. The solid fraction was washed five times with distilled water following the sequence of mixing, settling, and decanting. The last suspension was filtered, and the residual solid was then dried at 105 º C, ground in a mortar, and sieved through a 200 mesh sieve. The product was used in the study.

The average chemical composition of red mud was listed in Table 1. This table showed that red mud is primarily a mixture of Ca, Si, Fe and Al oxides and the CaO content is the highest. The single-point N_2-BET method indicated that the specific surface area of a typical red mud sample was about 8.12m^2/gr. The red mud agglomerates by many small compact particles as shown by SEM in Fig. 1. According to the XRD pattern shown in Fig. 2, the identified mineral phases in the red mud are mainly gibbsite [$Al(OH)_3$], cristobalite [SiO_2], hematite [Fe_2O_3], calcium carbonate [$CaCO_3$], sodium oxide [Na_2O], periclase [MgO] and anatase [TiO_2].

ISSN 2291-6458 (Print), ISSN 2291-6466 (Online)
Year 2014 | Volume 2 | Issue 1 | Page 83-96

Table 1. Chemical analysis characterization of Red mud

Chemical analysis of red mud							
Composition (wt%)	CaO	Al_2O_3	SiO_2	Fe_2O_3	Na_2O	MgO	TiO_2
	24.0	19.0	18.8	15.7	7.8	6.6	6.4

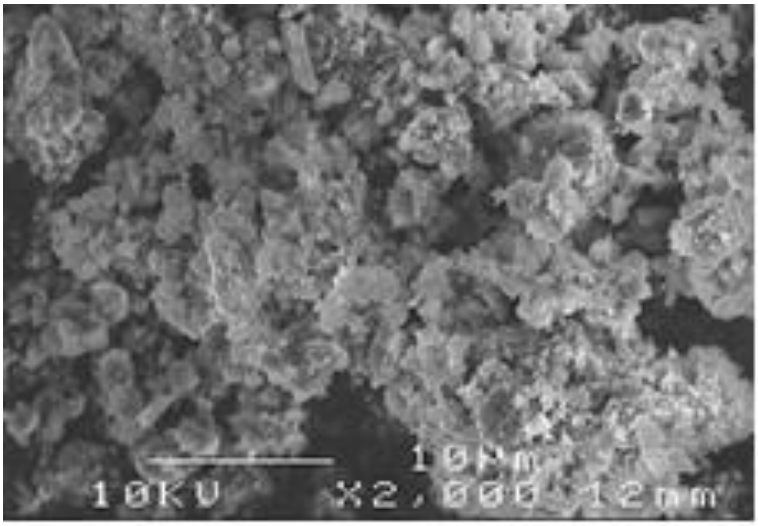

Figure 1. SEM images of red mud

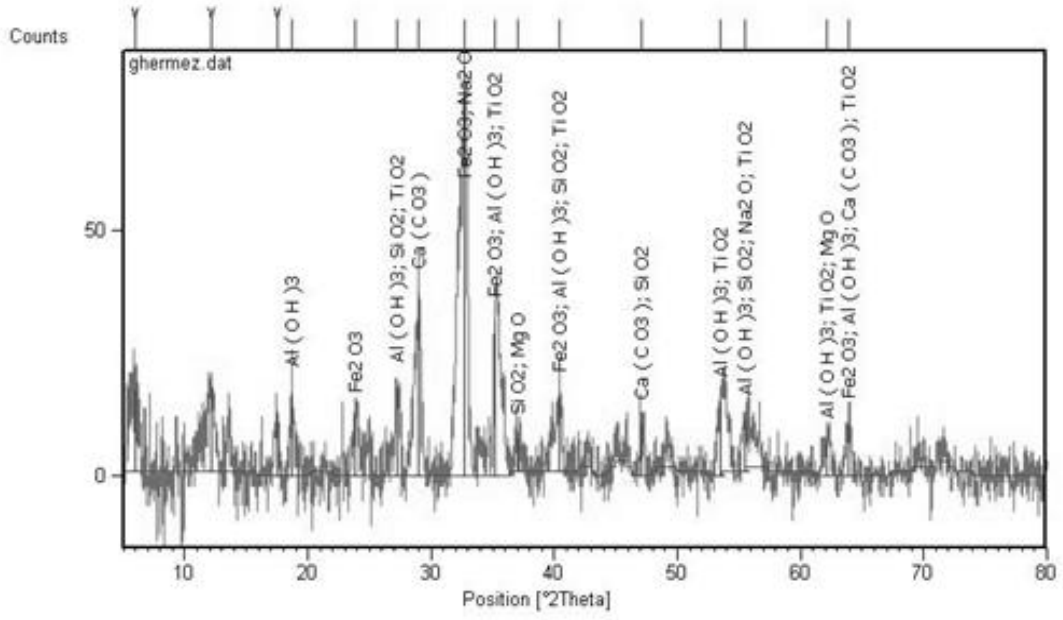

Figure 2. XRD pattern of red mud

ISSN 2291-6458 (Print), ISSN 2291-6466 (Online)
Year 2014 | Volume 2 | Issue 1 | Page 83-96

2.2. Batch adsorption experiments

Aqueous solutions containing Pb^{2+} ions of concentration 30, 40, 50 and 100 mg/L were prepared from Lead nitrate ($Pb(NO_3)_2$, Merck No.7397). 1 g of red mud was introduced in a stirred tank reactor containing 500 ml of the prepared solution. The stirring speed of the agitator was 300 rpm. The temperature of the suspension was maintained at 20 ±1 ° C. The initial pH of the solution was adjusted to the value 7.5 by adding NH_3 and HCl. Samples were taken after mixing the adsorbent and Pb^{2+} ion bearing solution at pre determined time intervals (5, 10, 20, 30, 60, and 120 min) for the measurement of residual metal ion concentration in the solution and to ensure equilibrium was reached. After specified time the sorbents were separated from the solution by centrifuge and filtration through the filter paper (Whatman grade6). The exact concentration of metal ions was determined by AAS (GBC 932 Plus atomic absorption spectrophotometer). All experiments were carried out twice. The mass balance of lead is given by:

$$mq = V(C_0 - C) \quad (1)$$

Where m is the weight of red mud (g), q the amount of lead removed by unit of weight of red mud (Uptake capacity: mg Pb/g red mud), V the volume of lead solution (L), C_0 the initial lead concentration of solution (mg Pb/L) and C is the concentration of lead at the time t of adsorption (mg Pb/L). After a long time (120 min), C and q will reach equilibrium value C_e and q_e.

2.3. Column adsorption experiments

Continuous flow adsorption experiments were conducted in glass columns of 1.0 cm inside diameter. At the top of the column, the influent lead solution (30, 40 and 50 mg Pb/L) was pumped through the packed column (5, 7 and 10 cm), at flow rates of 3, 5 and 7 mL/min, using a peristaltic pump. Samples were collected from the exit of the column at regular time intervals and analyzed for residual lead concentration (GBC 932 Plus atomic absorption spectrophotometer).

3. RESULTS AND DISCUSSION

3.1. Batch adsorption experiments

3.1.1. Effect of contact time and initial Pb^{2+} concentration

As shown in Fig. 3, the lead adsorption process took place in two stages. The first rapid stage in which 80–90% adsorption was achieved in 10 min, and a slower second stage, with equilibrium attained in 2 h. The first stage was due to the initial accumulation of lead at the red mud surface, as the relatively large surface area was utilized. With the increasing occupation of surface binding sites, the adsorption process slowed. The second stage was due to the penetration of lead ions to the inner active sites of the adsorbent. This concurs with the observations in similar studies [18, 19].

The sorption of Pb^{2+} cations was carried out at different initial lead concentrations ranging from 30 to 100 mg/L, at pH 7.5, at 300 rpm with 120 min of contact time using red mud. The uptake of the Pb^{2+} ion is increased by increasing the initial metal concentration tending to saturation at higher metal concentrations. As shown in Fig. 4.When the initial Pb^{2+} cations concentration increased from 30 to 100 mg/L, the uptake capacity of red mud increased from 12 to 18 mg/g. A higher initial concentration provided an important driving force to overcome all mass transfer resistances of the pollutant between the aqueous and solid phases thus increased the uptake [20].

3.1.2. Adsorption isotherms

Analysis of the equilibrium data is important to develop an equation which accurately represents the results and which could be used for design purposes [21]. Several isotherm equations have been used for the equilibrium modeling of adsorption systems. The sorption data have been subjected to different

ISSN 2291-6458 (Print), ISSN 2291-6466 (Online)
Year 2014 | Volume 2 | Issue 1 | Page 83-96

sorption isotherms, namely, Langmuir, and Freundlich. The equilibrium data for lead cations over the concentration range from 30 to 100 mg/L at 20°C have been correlated with the Langmuir isotherm [22]:

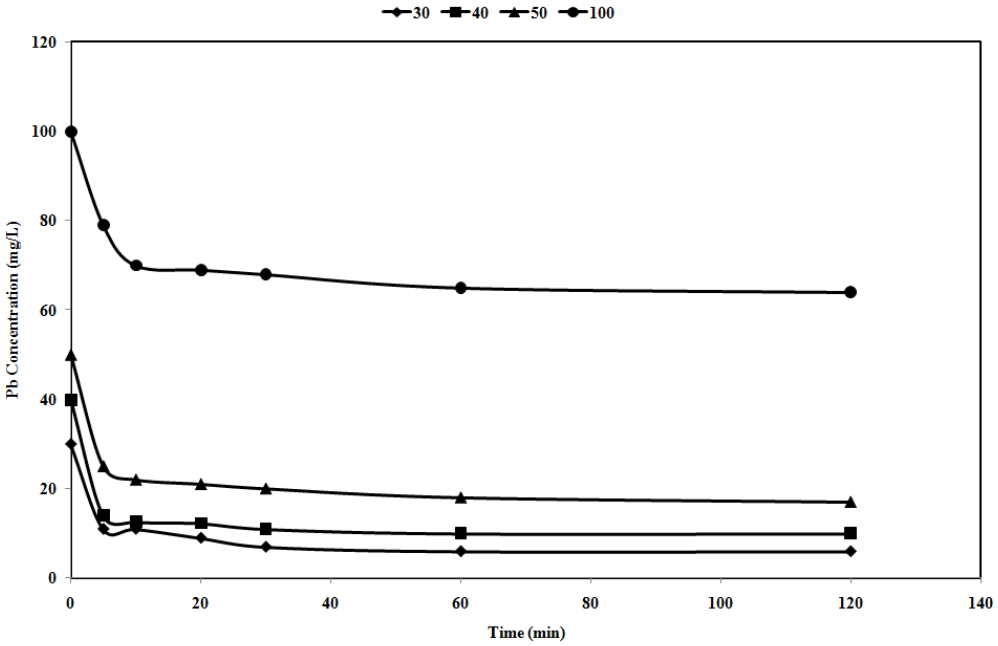

Figure 3. Effect of initial concentration of lead on adsorption as a function of contact time

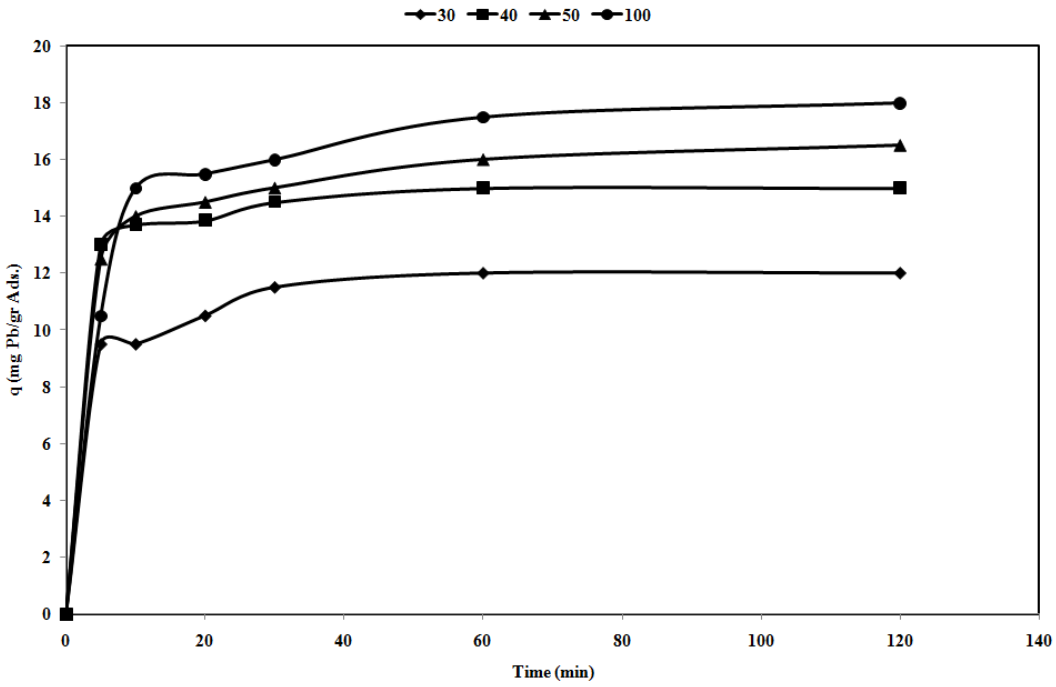

Figure 4. Effect of initial concentration on removal of Pb^{2+} by red mud sorbents (pH 7.5, adsorbent dosage = 2gr/L, 300rpm agitating rate)

ISSN 2291-6458 (Print), ISSN 2291-6466 (Online)
Year 2014 | Volume 2 | Issue 1 | Page 83-96

$$\frac{C_e}{q_e} = \frac{1}{Q_0 K} + \frac{C_e}{Q_0} \qquad (2)$$

Where C_e is the equilibrium concentration of lead in solution (mg/L), q_e is the amount absorbed at equilibrium onto red mud (mg/g), Q_0 and K are Langmuir constants related to sorption capacity and sorption energy, respectively. Maximum sorption capacity (Q_0) represents monolayer coverage of sorbent with sorbate and K represents enthalpy of sorption and should vary with temperature. A linear plot is obtained when C_e/q_e is plotted against C_e over the entire concentration range of metal ions investigated.
The linearized Langmuir adsorption isotherms of Pb^{2+} ions are given in Fig.5. (a). An adsorption isotherm characterized by certain constants which values express the surface properties and affinity of the sorbent and can also be used to find the sorption capacity of sorbent.

The Freundlich sorption isotherm, one of the most widely used mathematical descriptions, usually fits the experimental data over a wide range of concentrations. This isotherm gives an expression encompassing the surface heterogeneity and the exponential distribution of active sites and their energies. The Freundlich adsorption isotherms were also applied to the removal of Pb^{2+} on red mud (Fig.5. (b)).

$$Ln\, q_e = Ln\, k_f + \frac{1}{n} Ln\, C_e \qquad (3)$$

Where q_e is the amount of metal ion sorbed at equilibrium per gram of adsorbent (mg/g), C_e the equilibrium concentration of metal ion in the solution (mg/L), k_f, and n the Freundlich model constants [23, 24]. Freundlich parameters, k_f and n, were determined by plotting ln q_e versus ln C_e. The numerical value of $1/n < 1$ indicates that adsorption capacity is only slightly suppressed at lower equilibrium concentrations. This isotherm does not predict any saturation of the sorbent by the sorbate; thus infinite surface coverage is predicted mathematically, indicating multilayer adsorption on the surface [25].

The Langmuir and Freundlich adsorption constants from the isotherms and their correlation coefficients are also presented in Table.2. The correlation factors R (0.999, and 0.802 for Langmuir, and Freundlich model, respectively) confirm good agreement between both theoretical models and our experimental results. The maximum sorption capacity, Q_0, calculated from Langmuir equation is 18.87 mg/g, while Langmuir constant K is 0.35 L/mg. The values obtained for Pb^{2+} from the Freundlich model showed a maximum adsorption capacity (K_f) of 9.93 mg/g with an affinity value (n) equal to 6.53.
The values indicate that the adsorption pattern for Pb^{2+} on red mud followed second the Langmuir isotherm ($R^2 > 0.999$), and the Freundlich isotherm ($R^2 > 0.802$) at all experiments.

Table 2: Langmuir and Freundlich isotherm parameters for the adsorption of lead on red mud.

Langmuir isotherm		Freundlich isotherm	
Q_0(mg/g)	18.87	K_f(mg/g)	9.93
K(L/mg)	0.35	n	6.53
R^2	0.999	R^2	0.802

ISSN 2291-6458 (Print), ISSN 2291-6466 (Online)
Year 2014 | Volume 2 | Issue 1 | Page 83-96

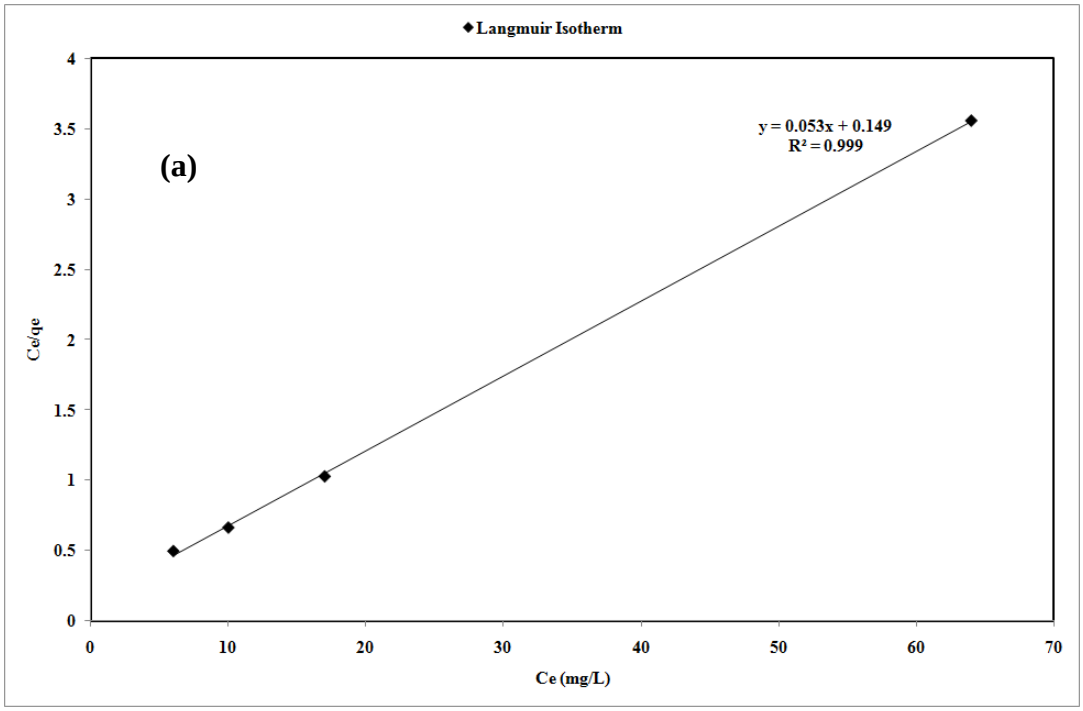

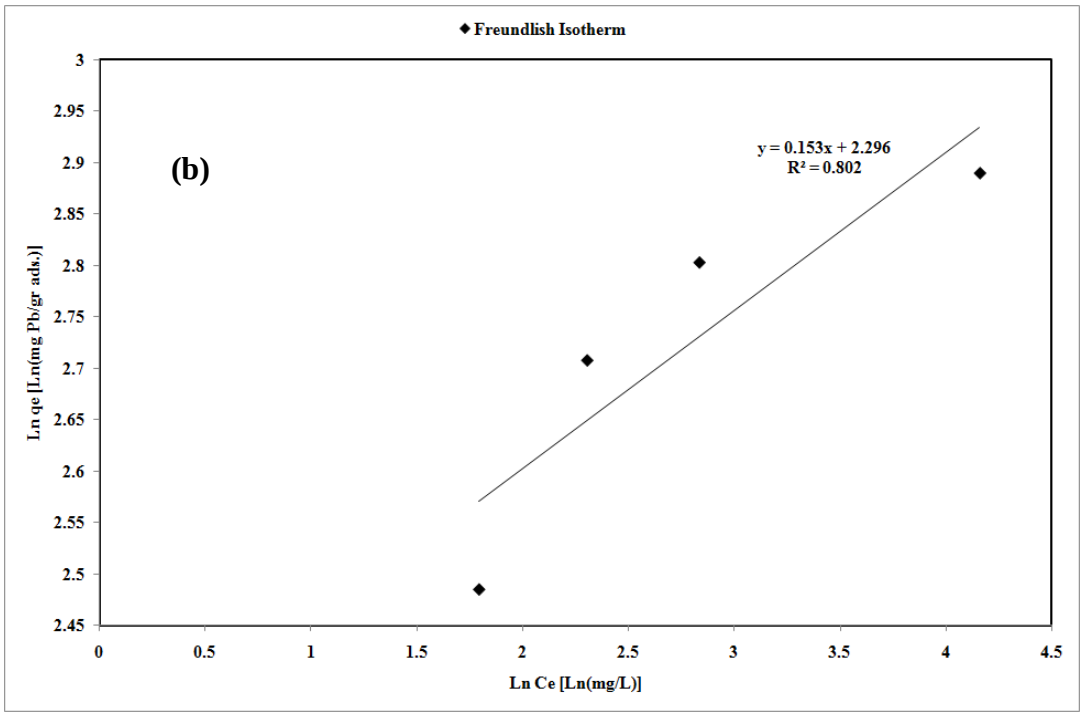

Figure 5. (a) Langmuir and (b) Freundlich plots for lead adsorption on red mud (initial pH 7.5, equilibrium contact time 2 h, adsorbent dosage 2 g/L, 300rpm agitating rate and temperature 20 ° C)

ISSN 2291-6458 (Print), ISSN 2291-6466 (Online)
Year 2014 | Volume 2 | Issue 1 | Page 83-96

It is clear that the Langmuir isotherm has best fitted for the sorption of Pb^{2+} on red mud. When the system is in a state of equilibrium, the distribution of Pb^{2+} between the red mud and the Pb^{2+} solution is of fundamental importance in determining the maximum sorption capacity of red mud for the Pb^{2+} ion from the isotherm.

The values of the maximum adsorption capacities for the adsorption of Pb^{2+} cations on different adsorbents used in the literature with adsorbent of the present study are summarized in Table 3. Although direct comparison of the red mud with other adsorbent materials is difficult, owing to the differences in experimental conditions, it was found that the maximum adsorption capacity of Jajarm red mud was 18.87 mg/g.

Table 3: Adsorption capacities of various adsorbents

Adsorbents	Adsorption capacity (mg/g)	Reference
Palm shell AC	95.20	[26]
Iron slag	17.20	[26]
RS1301	95.24	[26]
Rice husk	120.48	[27]
Peanut husk	29.14	[27]
Spent grain	35.5	[27]
Nipah palm shoot biomass	52.86	[27]
ZnO	6.70	[28]
Sawdust (pinus sylvestris)	9.78	[27]
Walnut sawdust	4.48	[27]
Bagasse fly ash	2.50	[27]
Jagarm red mud	18.87	Present work

3.2. Column adsorption experiments

3.2.1 Effect of flow rate

The adsorption columns were operated with different flow rates (5, 7 and 10 mL/min) until no further lead removal was observed. The breakthrough curve for a column was determined by plotting the ratio of the C_e/C_0 (C_e and C_0 are the lead concentrations of effluent and influent, respectively) against time, as shown in Fig. 6. The column performed well at the lowest flow rate (5 mL/min). Earlier breakthrough and exhaustion times were achieved, when the flow rate was increased from 5 to 10 mL/min. The column breakthrough time (C_e/C_0=0.05) was reduced from 12 to 4 min, with an increase in flow rate from 5 to 10 mL/min. This was due to a decrease in the residence time, which restricted the contact of lead solution to the red mud. At higher flow rates the lead ions did not have enough time to diffuse into the pores of the red mud and they exited the column before equilibrium occurred. Similar results have been found for As (III) removal in a fixed-bed system using modified calcined bauxite and for color removal in a fixed-bed column system using surfactant-modified zeolite [29, 30].

3.2.2 Effect of initial Lead concentration

The adsorption breakthrough curves obtained by changing initial lead concentration from 30 to 50 mg Pb/L at 5 mL/min flow rate and 50 mm bed depth are given in Fig. 7. As expected, a decrease in lead concentration gave a later breakthrough curve; the treated volume was greatest at the lowest transport due to a decreased diffusion coefficient or mass transfer coefficient [31]. Breakthrough time (C_e/C_0=0.05) occurred after 16.5 min at 30 mg/L initial lead concentration while the breakthrough time was 8 min at 50

ISSN 2291-6458 (Print), ISSN 2291-6466 (Online)
Year 2014 | Volume 2 | Issue 1 | Page 83-96

mg/L. The breakthrough time decreased with increasing lead concentration as the binding sites became more quickly saturated in the column.

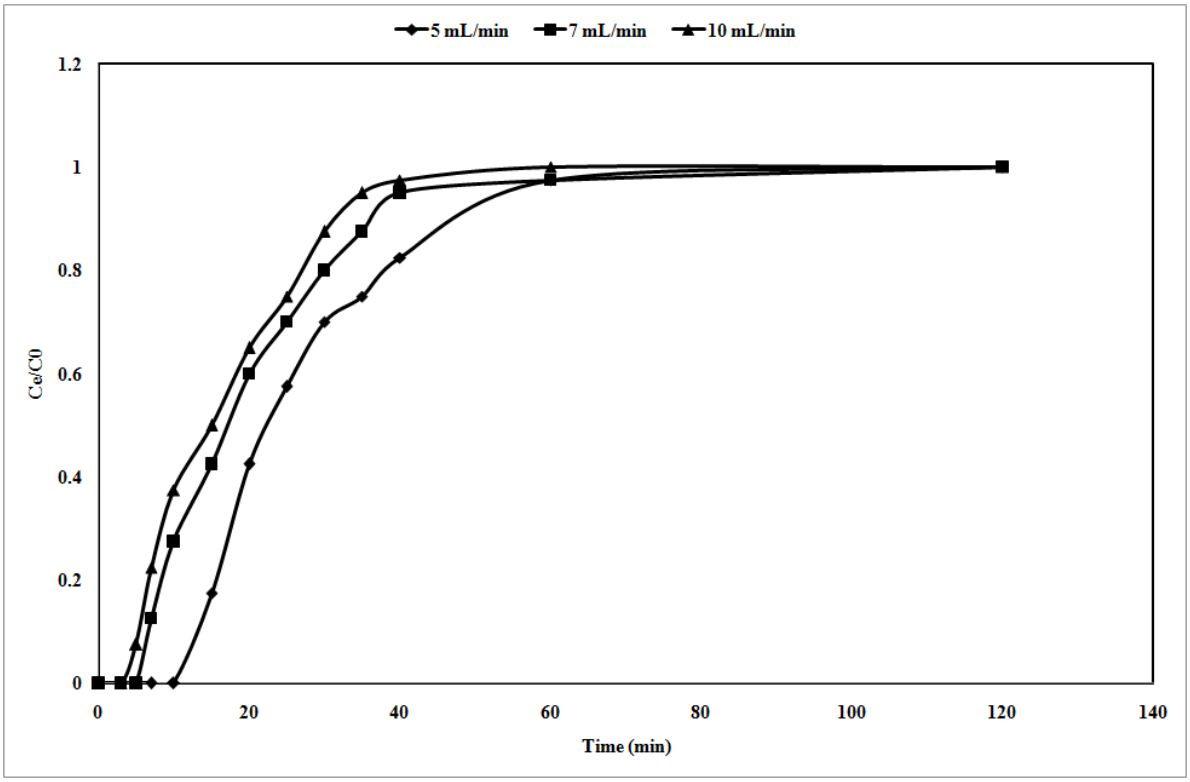

Figure 6. Breakthrough curves expressed as C_e/C_0 versus time at different flow rates (initial lead concentration 40 mg/L, initial pH 7.5, bed depth 50 mm and temperature 20 ±1°C)

Successful design of a column lead adsorption process requires a description of the dynamic behavior of lead ion in a fixed bed. Various simple mathematical models have been developed to describe and possibly predict the dynamic behavior of the bed in column performance [32]. One model used for continuous flow conditions is the Thomas model [33], which can be written as:

$$\ln\left(\frac{C_0}{C_t}-1\right)=\frac{k_{th}q_0m}{Q}-k_{th}C_0t \qquad (4)$$

where, k_{th} is the Thomas model constant (L/mg h), q_0 is the adsorption capacity (mg/g), Q is the volumetric flow rate through column (L/h),m is the mass of adsorbent in the column (g), C_0 is the initial lead concentration (mg/L) and C_e is the effluent lead concentration (mg/L) at any time t (h). The Thomas model constants k_{th} and q_0 were determined from a plot of ln [C_0/C_e−1] versus t at a given flow rate. The model parameters are given in Table 4. The Thomas model gave a good fit of the experimental data, at all the flow rates examined, with correlation coefficients greater than 0.970, which would indicate that the external and internal diffusions were not the rate limiting step [32]. The rate constant (k_{th}) decreased with increasing initial Lead concentration which indicates that the mass transport resistance increases. The reason is that the driving force for adsorption is the lead concentration difference between red mud and

ISSN 2291-6458 (Print), ISSN 2291-6466 (Online)
Year 2014 | Volume 2 | Issue 1 | Page 83-96

solution [32, 34].

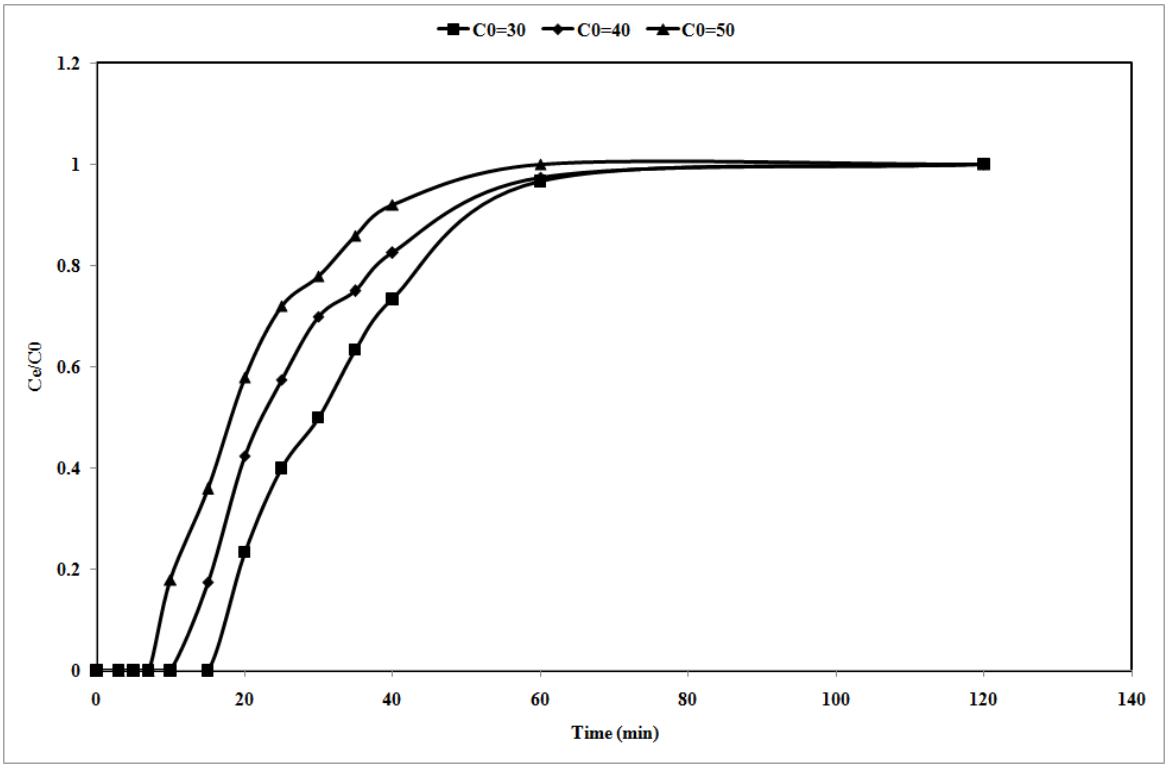

Figure 7. Breakthrough curves expressed as C_e/C_0 versus time at different lead concentrations (initial pH 7.5, flow rate 5 mL/min, bed depth 50 mm and temperature 20 ±1°C)

Table 4. The Thomas model and BDST model parameters for the adsorption of lead on red mud

The Thomas model parameters			
Lead concentration (mg/L)	q_0 *(mg/g)*	k_{th} (L/mg h)	R^2
30	54.06	0.0037	0.996
40	59.14	0.0027	0.970
50	59.30	0.0025	0.976
The BDST model parameters			
N (mg/L)	K_α (L/mg h)		R^2
360.26	0.5936		0.868

ISSN 2291-6458 (Print), ISSN 2291-6466 (Online)
Year 2014 | Volume 2 | Issue 1 | Page 83-96

3.2.3 Effect of bed height

The accumulation of lead in a fixed-bed column is dependent on the quantity of adsorbent inside the column. In order to study the effect of bed height on lead retention, red mud of three different bed heights, viz. 50, 70, and 100 mm, were used. A lead solution of fixed concentration (40 mg Pb/L) was passed through the fixed-bed column at a constant flow rate of 5 mL/min. As depicted by Fig. 8 the breakthrough time varied with bed height. Steeper breakthrough curves were achieved with a decrease in bed depth. The breakthrough time decreased with a decreasing bed depth from 100 to 50 mm, as binding sites were restricted at low bed depths. At low bed depth, the lead ions do not have enough time to diffuse into the surface of the red mud, and a reduction in breakthrough time occurs. Conversely, with an increase in bed depth, the residence time of lead solution inside the column was increased, allowing the lead ions to diffuse deeper into the red mud.

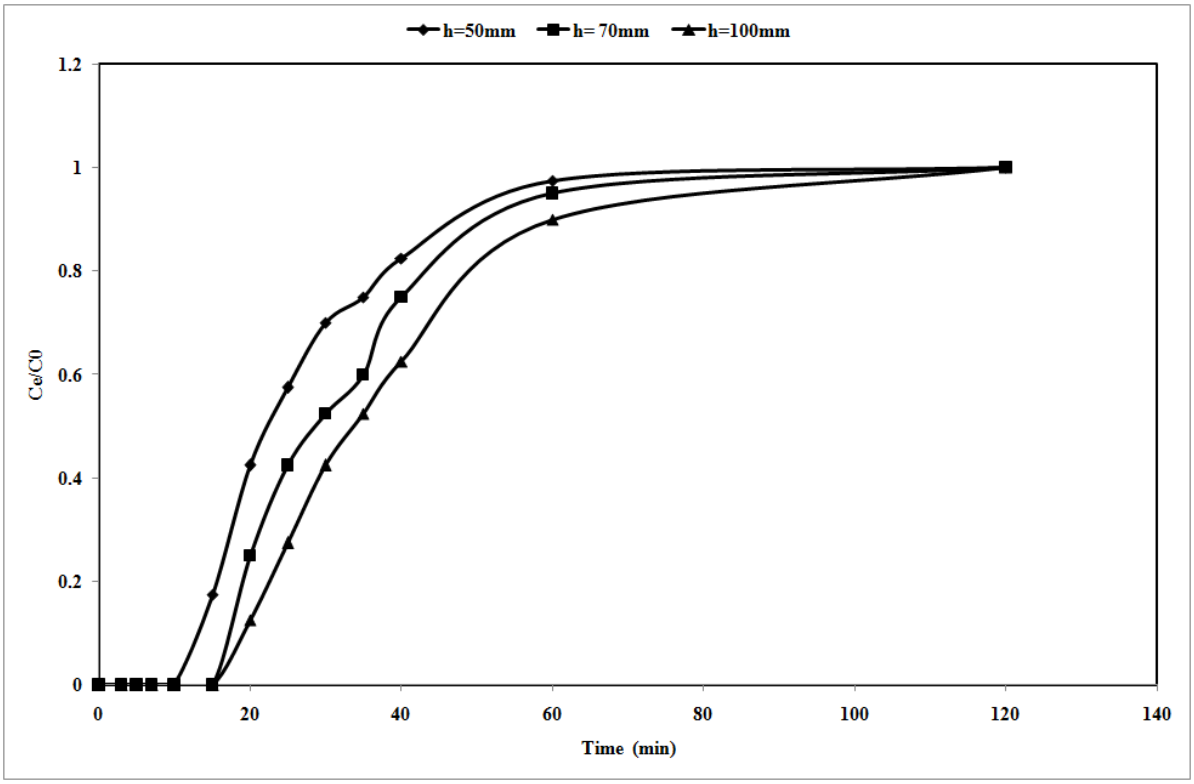

Figure 8. Breakthrough curves expressed as C_e/C_0 versus time at different bed depth (initial lead concentration 40 mg/L, initial pH 7.5, flow rate 5 mL/min and temperature 20 ±1°C)

The breakthrough service time (BDST) model is based on physically measuring the capacity of the bed at various percentage breakthrough values. The BDST model constants can be helpful to scale up the process for other flow rates and concentrations without further experimentation. It is used to predict the column performance for any bed length, if data for some depths are known. It states that the bed depth, Z and service time, t of a column bears a linear relationship. The rate of adsorption is controlled by the surface reaction between adsorbate and the unused capacity of the adsorbent.

ISSN 2291-6458 (Print), ISSN 2291-6466 (Online)
Year 2014 | Volume 2 | Issue 1 | Page 83-96

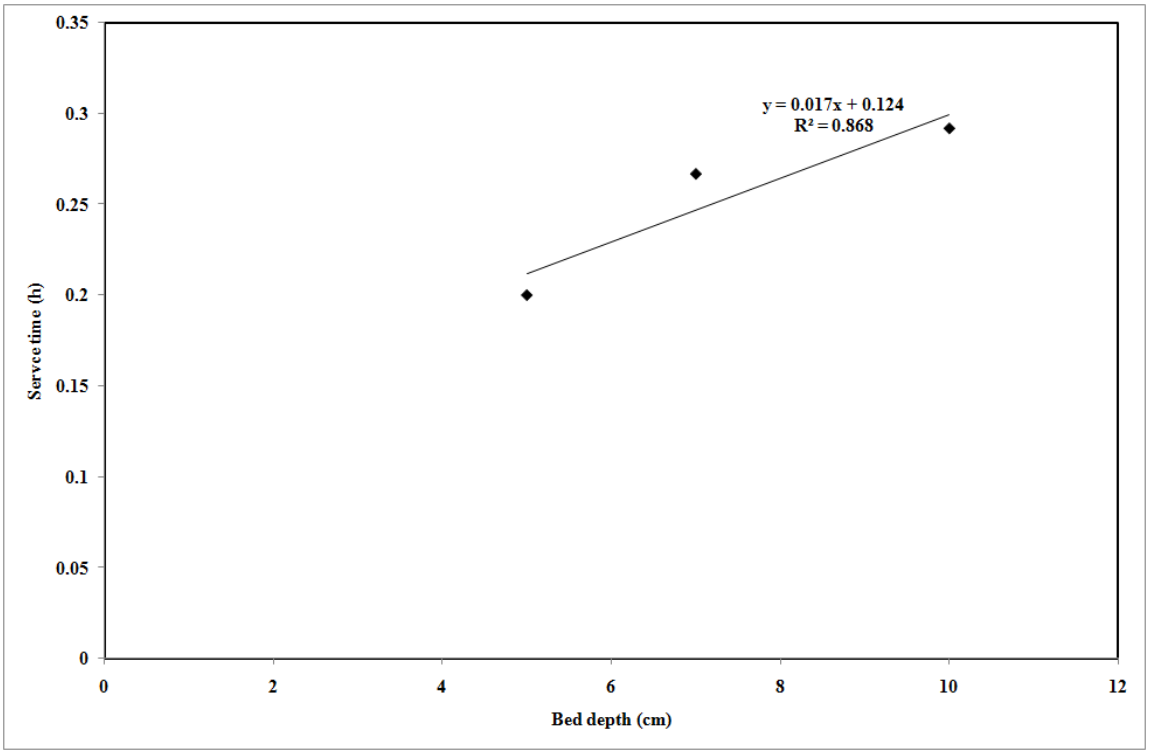

Figure 9. Plot of BDST equation for lead adsorption on red mud

The BDST equation can be expressed as follows [35]:

$$t = \frac{NZ}{C_0 v} - \frac{1}{K_\alpha C_0} Ln\left[\left(\frac{C_0}{C_b}\right) - 1\right] \qquad (5)$$

where C_b is the breakthrough lead concentration (mg/L), N is the adsorption capacity of bed (mg/L), Z is depth of column bed (cm), v is the linear flow velocity of lead solution through the bed (mL/cm^2 h), Kα is the rate constant (L/mg h). The column service time was selected as the time when the normalized concentration, C_e/C_0 reached 0.05. A plot of service time versus bed depth, at a flow rate of 5 mL/min (Fig. 9) was linear. The correlation coefficient value (R^2=0.868) indicated the validity of the BDST model for the present system. The values of BDST model parameters are presented in Table 4. The value of Kα characterizes the rate of transfer from the fluid phase to the solid phase. If Kα is large, even a short bed will avoid breakthrough, but as Kα decreases a progressively deeper bed is required to avoid breakthrough.

4. CONCLUSIONS

In this study, the lead adsorption capacity of red mud was evaluated for batch and fixed-bed column adsorption systems. Batch experiments indicated that the time to attain equilibrium was 2 h. The adsorption of lead on red mud in batch systems can be described by the Langmuir isotherm, and the adsorption capacity was 18.87 mg/g. The fixed-bed column breakthrough curves were analyzed at different flow rates, bed depth and initial lead concentration. Thomas and BDST models were successfully used for predicting breakthrough curves for lead removal by a fixed bed of red mud using

ISSN 2291-6458 (Print), ISSN 2291-6466 (Online)
Year 2014 | Volume 2 | Issue 1 | Page 83-96

different initial lead concentration and bed depths. Despite its slightly low performance, the use of red mud as an adsorbent for lead removal is potentially cost-effective and may provide an alternative method for lead removal from contaminated water.

REFERENCES AND NOTES

[1] Huang, X.; Sillanpëë, M.; Dou, B.; Gjessing, E. T. Water quality in the Tibetan Plateau: metal contents of four selected rivers, *Environ. Pollut*. **2008**, *156*, 270–277.

[2] Aman, T.; Kazi, A. A.; Sabri, M. U.,; Bano, Q. Potato peels as solid waste for the removal of heavy metal copper (II) from waste water/industrial effluent, *Colloids, Surf., B Bio interfaces.* **2008**, *63*, 116–121.

[3] Jiang, Y.; Pang, H.; Liao, B. Removal of copper (II) ions from aqueous solution by modified bagasse, *J. Hazard. Mater*. **2008**, *164*, 1–9.

[4] Vangronsveld, J.; Colpaert J.; Tichelen K.. V. Reclamation of a bare industrial area contaminated by non-ferrous metals: physicochemical and biological evaluation of the durability of soil treatment and revegetation, *Environ. Pollut*., **1995**, *94***,** 131-140.

[5] Mobasherpour, I.; Salahi, E.; Pazouki, M.; Potential of nano crystalline hydroxyapatite for lead (II) removal from aqueous solutions: Thermodynamic and Adsorption isotherm study, *African J. Pure Applied Chem*. **2011**, *5(11)*, 383-392,

[6] Ajmal, M.; Khan, A.H.; Ahmad, S. Role of sawdust in the removal of copper (II) from industrial wastes, *Water Res*. **1998**, *32*, 3085–3091.

[7] Donmez, G.; Aksu, Z. The effect of copper (II) ions on the growth and bioaccumulation properties of some yeasts, *Proc. Biochem*. **1999**, *35*, 135–142.

[8] Yu, B.; Zhang, Y.; Shukla, S. S. The removal of heavy metal from aqueous solutions by sawdust adsorption-removal of copper, *J. Hazard. Mater*. **2000**, *80*, 33–42.

[9] Virkutyte, J.; Hullebusch, E.; Sillanpëë, M.; Lens, P. Copper and trace element fractionation in electrokinetically treated anaerobic granular sludge, *Environ. Pollut*. **2005**, *138*, 518–529.

[10] Kalkan, E.; Akbulut, S. The positive effects of silica fume on the permeability, swelling pressure and compressive strength of natural clay liners, *Engineering Geology.* **2004**, *73*, 145–156.

[11] Kalkan, E. Influence of silica fume on the desiccation cracks of compacted clayey soils, *Appl. Clay Sci*. **2008**, *43*, 296–302.

[12] Zheng, W.; Li, X.; Wang, F.; Yanga, Q.; Dengb, P.; Zenga, G. Adsorption removal of cadmiumand copper fromaqueous solution by areca—a foodwaste, *J.Hazard.Mater*. **2008**, *157*, 490–495.

[13] Poulin, E.; Blais, J.F.; Mercier, G. Transformation of red mud from aluminium industry into a coagulant forwastewater treatment, *Hydrometallurgy*. **2008**, *92 (1–2)*,16–25.

[14] Gupta, V. K.; Gupta, M.; Sharma, S. Process development for the removal of lead and chromium from aqueous solutions using red mud—an aluminum industry waste, *Water Res*. **2001**, *35(5)*, 1125–1134.

[15] Pradhan, J.; Das, S. N.; Thakur, R.S. Adsorption of hexavalent chromium from aqueous solution by using activated red mud, *J. Colloid Interf. Sci*. **1999**, *217(1)*, 137–141.

[16] Wang, S. B.; Boyjoo, Y.; Choueib, A.; Zhu, Z.H. Removal of dyes from aqueous solution using fly ash and red mud, *Water Res.* **2005**, *39(1)*, 129–138.

[17] Wang, S.; Ang, H. M.; Tadé, M.O. Novel applications of red mud as coagulant, adsorbent and catalyst for environmentally benign processes, *Chemosphere.* **2008**, *72(11)*, 1621–1635.

[18] Qaiser, S.; Saleemi, A. R.; Umar, M. Biosorption of lead from aqueous solution by Ficus religiosa leaves: batch and column study, *J. Hazard. Mater*. **2009**, 166, 998–1005.

[19] Sangi, M. R.; Shahmoradi, A.; Zolgharnein, J.; Azimi, G. H.; Ghorbandoost, M. Removal and recovery of heavy metals from aqueous solution using Ulmus carpinifolia and Fraxinus excelsior tree leaves, *J. Hazard. Mater*. **2008**, *155*, 513–522.

[20] Aksu, Z.; Tezer, S. Biosorption of reactive dyes on the green alga Chlorella vulgaris. *Process Biochem*. **2005**, *40*, 1347–1361.

ISSN 2291-6458 (Print), ISSN 2291-6466 (Online)
Year 2014 | Volume 2 | Issue 1 | Page 83-96

[21] Aksu, Z. Determination of the equilibrium, kinetic and thermodynamic parameters of the batch biosorption of nickel(II) ions onto Chlorella vulgaris, *Process Biochem.*, **2002**, *38***,** 89-99.
[22] Langmuir, I. The adsorption of gases on plane surfaces of glass, mica and platinum, *J. Am. Chem. Soc.*, **1918**, *40***,** 1361-1403.
[23] Malkoc, E.; Nuho˘glu, Y. The removal of chromium(VI) from synthetic wastewater by Ulothrix zonata. *Fres. Environ. Bull.*, **2003**, *12***,** 376-381.
[24] Kadirvelu, K..; Thamaraiselvi, K.; Namasivayam, C. Adsorption of nickel(II) from aqueous solution onto activated carbon prepared from coirpith, *Sep. Purif. Technol.*, **2001**, *24***,** 497-505.
[25] Hasany, S. M.; Saeed, M. M.; Ahmed, M.; Radioanal, J. Sorption and thermodynamic behavior of zinc(II)-thiocyanate complexes onto polyurethane foam from acidic solutions, *Nucl. Chem.*, **2002**, *252***,** 477-484.
[26] Gadupudi Purnachadra, R., Chungsying, L., Fengsheng, S.: Sorption of divalent metal ions from aqueous solution by carbon nanotubes: A review, *Sep. Purif. Technol*, **2007**, *58*, 224-231.
[27] Wan Ngah, W.S., Hanafiah, M.A.K.M.: Removal of heavy metal ions from wastewater by chemically modified plant wastes as adsorbents: A review, *Bioresource Technol*, **2008**, *99*, 3935–3948.
[28] Ming, H., Shujuan, Z., Bingcai, P., Weiming, Z., Lu, L., Quanxing, Z.,: Heavy metal removal from water/wastewater by nanosized metal oxides: A review, *J. Hazard. Mater.* **2012**, *211-212*, 317-331.
[29] Bhakat, P. B.; Gupta, A. K.; Ayoob, S. Feasibility analysis of As (III) removal in a continuous flow fixed-bed system by modified calcined bauxite (MCB), *J. Hazard. Mater*. **2007**, *139*, 286–292.
[30] Ozdemir, O.; Turan, M.; Turan, A. Z.; Faki, A.; Engin, A. B. Feasibility analysis of color removal from textile dyeing wastewater in a fixed-bed column system by surfactant-modified zeolite (SMZ), *J. Hazard. Mater*. **2009**, *166*, 647–654.
[31] Uddin, M. T.; Rukanuzzaman, M.; Khan, M. M.; Islam, M. A. Adsorption of methylene blue from aqueous solution by jackfruit (Artocarpus heteropyllus) leaf powder: a fix-bed column study, *J. Environ. Manage*. **2009**, *90*, 3443–3450.
[32] Aksu, Z.; Gonen, F. Bisorption of phenol by immobilized activated sludge in a continuous packed bed: prediction of breakthrough curves, *Process Biochem*. **2004**, *39*, 599–613.
[33] Thomas, H. C. Heterogeneous ion exchange in a flowing system, *J. Am. Chem. Soc*. **1944**, 66, 1664–1666.
[34] Han, R. P.; Zhang, J. H.; Zou, W. H.; Xiao, H. J.; Shi, J.; Liu, H. M. Biosorption of copper (II) and lead (II) from aqueous solution by chaff in a fixed-bed column, *J. Hazard. Mater*. **2006**, *133*, 262–268.
[35] Hutchins, R. A. New methods simplifies design of activated carbon system, *Chem.Eng*. **1973**, *80*, 133–138.

The authors declare no conflict of interest

© 2014 By the Authors; Licensee Borderless Science Publishing, Canada. This is an open access article distributed under the terms and conditions of the Creative Commons Attribution license http://creativecommons.org/licenses/by/3.0/